

for lattice melting, evidence was seen of molten crystal "squirting" out the channel at the contacts, Fig. 7.

Were the carrier concentrations as low as the estimates given by Osipov and Khvoschchev,⁶ who did not take into account thermal ionization, the theoretical curves in Fig. 5 would be moved up the ordinate by a factor of ~ 6 . The conclusions to be drawn from the agreement between the theoretical curves and the experimental points is 1) that thermal ionization takes place within the time ($\sim 0.05 \mu\text{sec}$) required for Bennett pinching to occur and 2) that a different kind of pinching or thermoelectric instability has been observed which continually enhances the current flowing in an extremely narrow channel in a semiconductor. This may be contrasted with an equilibrium model⁷ in which thermal conduction just balances joule heating. An analog computer study using parameters appropriate

to the materials of the present experiments has shown that an equilibrium thermal pinch at these temperatures would have a radius about half the sample radius and at least an order of magnitude larger than those observed. This present thermal pinch effect is initiated by Bennett's pinch effect but dominates the conduction immediately after the onset of pinching and for the entire remainder of the pulse ($\sim 99\%$ of the pulse time). The necessary critical condition for the onset of the instability is that after initiation the power into the pinch less the heat conduction loss be greater than zero.

ACKNOWLEDGMENTS

During this work we were aided by helpful discussions with R. W. Cunningham, and the expert technical assistance of R. W. Boice and M. F. Berg.

Interband Faraday Rotation in Germanium

D. L. MITCHELL AND R. F. WALLIS

U. S. Naval Research Laboratory, Washington, D. C.

(Received 5 December 1962; revised manuscript received 22 March 1963)

The room-temperature Faraday rotation of germanium has been measured in magnetic fields ranging from 0 to 120 kG for a range of photon energies above and below the band-gap energy at $\mathbf{k}=0$. Evidence for the possible influence of exciton transitions is found in both the weak- and strong-field cases. Saturation of the rotation in large fields is observed at photon energies near the zero-field direct band-gap energy. Certain effects of crystal strain are also observed.

I. INTRODUCTION

THE weak-field Faraday rotation in germanium has been measured by Hartmann and Kleman,¹ by Moss and Walton,² and more recently by Piller and Patton.³ The measurements show a reversal in sign and rapid increase in the magnitude of the rotation as the photon energy approaches the energy for direct interband transitions at $\mathbf{k}=0$ ($\hbar\omega < E_g$). Unfortunately, the earlier measurements are of limited precision in this region and also do not extend to energies above the band gap so that the exact form of the rotation in this region is not revealed. Recently, Nishina, Kolodziejczak, and Lax⁴ have reported measurements in strong magnetic fields which exhibit structure at photon energies larger than the band gap ($\hbar\omega > E_g$).

Theoretical treatments of the Faraday rotation arising from interband transitions have been given by

several authors.⁵⁻⁸ These treatments are based on a model which involves transitions between Landau levels and do not explicitly account for effects arising from the Coulomb interaction of electrons and holes. Such treatments might be expected to apply at photon energies much less than E_g . At photon energies near E_g , the theoretical work of Elliott⁹ and the experimental work of Macfarlane, McLean, Quarrington, and Roberts¹⁰ on germanium have shown that the zero magnetic-field absorption due to direct transitions is significantly modified by exciton effects. Furthermore, in strong magnetic fields the theoretical work of Elliott and Loudon¹¹ and the experimental work of Edwards and

⁵ M. Suffczynski, Proc. Phys. Soc. (London) **77**, 1042 (1961).

⁶ B. Lax and Y. Nishina, J. Appl. Phys. **32**, 2128 (1961).

⁷ I. M. Boswarva, R. E. Howard, and A. B. Lidiard, Proc. Roy. Soc. (London) **A269**, 125 (1962).

⁸ J. Kolodziejczak, B. Lax, and Y. Nishina, Phys. Rev. **128**, 2655 (1962).

⁹ R. J. Elliott, Phys. Rev. **108**, 1384 (1957).

¹⁰ G. G. Macfarlane, T. P. McLean, J. E. Quarrington, and V. Roberts, Proc. Phys. Soc. (London) **71**, 863 (1958).

¹¹ R. J. Elliott and R. Loudon, J. Phys. Chem. Solids **15**, 196 (1960). See also H. Hasegawa and R. E. Howard, *ibid.* **21**, 179 (1961).

¹ B. Hartmann and B. Kleman, Arkiv Fysik **18**, 75 (1960).

² A. K. Walton and T. S. Moss, Proc. Phys. Soc. (London) **78**, 1393 (1961).

³ H. Piller and V. A. Patton, Phys. Rev. **129**, 1169 (1963).

⁴ Y. Nishina, J. Kolodziejczak and B. Lax, Phys. Rev. Letters **9**, 55 (1962).

Lazazzera¹² have shown that discrete exciton transitions are dominant. The strong-field region is defined by the condition $\hbar\omega_{\text{ex}} \ll \hbar\omega_c$, where $\hbar\omega_{\text{ex}}$ is the exciton binding energy and ω_c is the cyclotron frequency determined with the reduced effective mass. For photon energies near to or greater than E_g , predictions based on Landau transitions should, therefore, not be expected to be entirely correct.

In order to investigate the possible influence of the exciton transitions, we have measured the room temperature Faraday rotation in weak magnetic fields ($\hbar\omega_{\text{ex}} \gg \hbar\omega_c$) at photon energies above and below the interband transition energy at $\hbar\omega_g$. We have also measured the strong-field ($\hbar\omega_{\text{ex}} \ll \hbar\omega_c$) Faraday rotation and related ellipticity over a similar range of photon energies.

II. EXPERIMENTAL METHOD

The measurement of the Faraday effect, Voigt effect, and similar experiments involves the measurement of the rotation of the plane of polarization and the ellipticity produced by the transmission of radiation through a sample placed in an external magnetic field. An ac system has been developed to measure and continuously record each of these quantities. The system offers the advantages inherent with an ac system, e.g., improvement of sensitivity by the use of detectors whose signal-to-noise ratio improves with frequency; increase in the speed and ease of measurement; stability and freedom from drift. A short description of the system will be given. The details will be published elsewhere.

Initially unpolarized radiation is passed through a sheet polarizer rotating at an angular frequency ω_1 . The polarized beam is then split into two components. One beam, the reference beam, is passed through a fixed polarizer, mounted in a divided circle, and is detected by a lead sulphide detector. The resulting signal of frequency $2\omega_1$ has a fixed phase relative to the angular setting of the reference polarizer. The second polarized beam passes through the sample, through another fixed polarizer, and into a grating monochromator where it is detected. The phase of this ac signal depends directly on the rotation of the plane of polarization within the sample and is independent of the ellipticity. The two signals are then amplified, filtered, and fed into a phase meter which may be calibrated to read directly the rotation in the sample. The output of the phase meter is recorded on an x - y recorder as a function of the wavelength or of the magnetic field.

To measure ellipticity produced by the sample, a chopper with a frequency ω_2 somewhat greater than ω_1 is placed in the signal beam after it passes through the sample. The signal generated by the detector then has a carrier frequency ω_2 which is amplitude modulated at a frequency $2\omega_1$ by the rotating polarizer. This modu-

lated signal has frequency components ω_2 and $\omega_2 \pm 2\omega_1$. The amplitude of the sum and difference frequency terms depends on the degree of ellipticity produced by the sample; the amplitudes go to zero as the radiation approaches circular polarization. The measurement is accomplished by maintaining the amplitude of the carrier at a fixed level and recording the amplitude of the difference frequency term as it is selected by a wave analyzer. The intensity ellipticity may be determined from this trace.

The samples for these measurements were prepared by grinding and polishing thin sections from x-ray-oriented single-crystal germanium. Certain of the thinner sections were prepared with a glass backing while others were unmounted and annealed to reduce crystal strain. The thicknesses of the thinner sections (4–12 μ) were determined from the measured interference structure in the region of transparency of the crystals.

The samples were placed in the center of the N R L Bitter magnets with the field determined to $\pm 4\%$. The temperatures of the samples were determined within 1°C by a thermocouple mounted in close proximity to the sample. The data were adjusted to the common temperature of either 300 or 289°K by applying the energy shift $-0.4 \text{ meV}/^\circ\text{K}$ determined by Macfarlane, McLean, Quarrington, and Roberts.¹⁰

III. FARADAY ROTATION AND ELLIPTICITY

The rotation of the plane of polarization in a medium with an index of refraction n_- for right circularly polarized (rcp) radiation and index n_+ for left circularly (lcp) radiation is given by the expression,

$$\theta = (-\omega/2c)(n_+ - n_-)t, \quad (3.1)$$

where ω represents the angular frequency of the radiation, c the velocity of light, and t the distance traversed. Positive rotations correspond to counter-clockwise rotations when viewed against the direction of propagation. The convention for (lcp) and (rcp) corresponds to that given by Jenkins and White.¹³ This convention defines (rcp) as having the spatial profile of a right-handed screw. This corresponds to a clockwise rotation of the \mathbf{E} vector in time when viewed against the direction of propagation at a fixed point in space. Boswarva, Howard, and Lidiard⁷ define (lcp) and (rcp) in the opposite sense; however, their assignment of plus and minus also differs so that the equations have the same form as presented here.

The ellipticity of the radiation produced by the medium is related to the absorption coefficients α_+ and α_- for (lcp) and (rcp) radiation. The amplitude ellipticity is given by the expression

$$\epsilon = \tanh[(\alpha_+ - \alpha_-)t/4]. \quad (3.2)$$

¹² D. F. Edwards and V. J. Lazazzera, Phys. Rev. **120**, 420 (1960).

¹³ F. A. Jenkins and H. E. White, *Fundamentals of Optics* (McGraw-Hill Book Company, Inc., New York, 1960).

In these measurements the intensity ellipticity, or the square of the quantity ϵ , is measured so that the sign of ϵ is left undetermined.

The Faraday rotation and ellipticity are not independent quantities but may be related by the dispersion relations developed by Bennett and Stern¹⁴ as adapted by Boswarva, Howard, and Lidiard.⁷

$$\theta(\omega) = \frac{-\omega^2 t}{2\pi n_0} \int_0^\infty \frac{(n_+ \alpha_+ - n_- \alpha_-)}{\omega'(\omega'^2 - \omega^2)} d\omega'. \quad (3.3)$$

Equation (3.3) is limited to frequencies ω for which $|n_+ - n_-| \ll n_0$ and $k_0 |k_+ - k_-| \ll n_0 |n_+ - n_-|$, where n_0 and k_0 refer to the zero-field values for the index of refraction and extinction coefficient. In the present case, the index difference $|n_+ - n_-|$ was of the order 10^{-2} at the highest fields applied (10^5 G) so that the quantities n_+ and n_- in Eq. (3.3) may be replaced by the value n_0 for the index in zero field.

IV. WEAK-FIELD FARADAY ROTATION

A. Experimental Results

The measured Faraday rotation as a function of the magnetic field is shown in Fig. 1 for several fixed photon energies in the immediate vicinity of the direct band gap at $\mathbf{k}=0$. The sample shown was annealed and freely mounted. The magnetic field and the radiation were both directed along the $\langle 100 \rangle$ crystal axis.

The rotation at high magnetic fields exhibits a non-linear dependence on the magnetic field. This arises from the cyclotron shift of the individual energy levels at high fields and will be discussed later. The rotation at low magnetic fields does exhibit a region in which the rotation increases linearly with magnetic field. The weak-field Faraday rotation is defined in this region

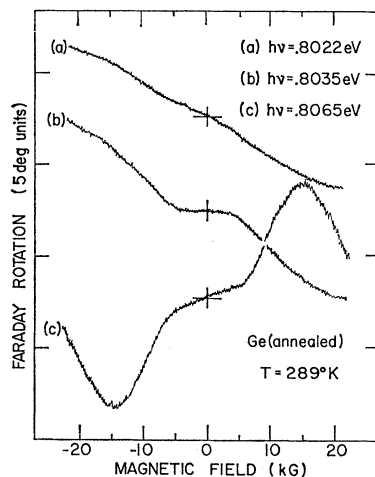


FIG. 1. Recorder traces of the Faraday rotation in germanium for weak magnetic fields. The fixed photon energies lie in the region of the direct interband transitions at $\mathbf{k}=0$.

¹⁴ H. S. Bennett and E. A. Stern, *Bull. Am. Phys. Soc.* **5**, 279 (1960). H. S. Bennett, Masters thesis, University of Maryland, 1960 (unpublished).

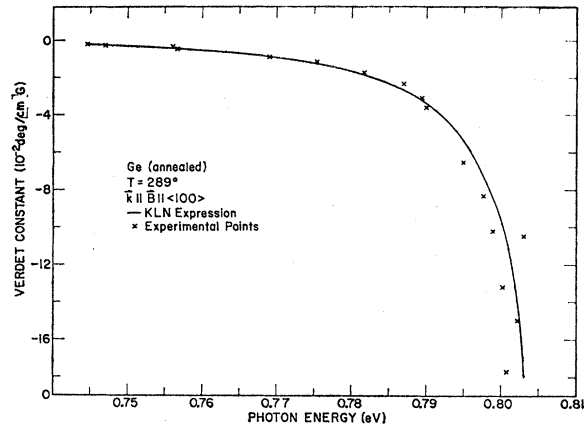


FIG. 2. Verdet constant of germanium for $\omega < \omega_g$. The fit to the theoretical curve is explained in the text. Note the turn-over of the experimental curve at the high-energy end of the curve.

and its value is taken from the slope of the rotation curve at zero field.

The Verdet constant obtained in this manner is plotted in Fig. 2 for photon energies less than the energy gap. The detailed structure of the Verdet constant in the immediate vicinity of the energy gap is shown in Fig. 3.

B. Discussion

A specific calculation of the Faraday rotation in germanium has been given by Suffczynski.⁵ His calculated value of 0.23 deg/cm-G for the peak rotation is in agreement with the experimentally observed value of 0.20 deg/cm-G; however, the approximations involved in the calculation indicate that the agreement is, at least, partly fortuitous.

More complete theories have been developed by Boswarva, Howard, and Lidiard⁷ and by Kolodziejczak, Lax, and Nishina.⁸ These authors have developed weak-field expressions for the Faraday rotation based on Landau transitions between simple parabolic bands. The expression given by Boswarva, Howard, and Lidiard⁷ may be obtained by inserting the expressions for α_{\pm} given by Elliott, McLean, and Macfarlane¹⁵ into the dispersion relation Eq. (3.3). The results of Kolodziejczak, Lax, and Nishina⁸ are obtained by a calculation of the conductivity tensor for a model consisting of classical oscillators. Both expressions have a dominating term of the form $(\omega_g - \omega)^{-1/2}$ at the frequencies just below the band-gap frequency ω_g .

We have plotted the expression given by Kolodziejczak, Lax, and Nishina⁸ as the solid line in Fig. 2. We have fixed the energy gap $E_g = 0.805$ eV as the best value from our experimental results. This is approximately 1 meV below the value quoted by Macfarlane, McLean, Quarrington, and Roberts¹⁰ at this temperature. The magnitude of the expression was adjusted to fit the

¹⁵ R. J. Elliott, T. P. McLean and G. G. Macfarlane, *Proc. Phys. Soc. (London)* **72**, 553 (1958).

experimental points at lower energies. The fit may be improved by shifting the assumed energy gap to lower energies as shown by Piller and Patton⁸; however, the value required to provide a proper fit lies below the accepted value by more than experimental error (± 1 meV).

The discrepancy, while not large, is appreciable in the immediate vicinity of the energy gap. One source for the discrepancy may be the neglect of the detailed band structure of germanium, which is not simple as assumed in the derivation of the theoretical expressions.

Another likely source is the modification of the transitions at the band edge produced by the Coulomb attraction between hole-electron pairs as suggested by Suffczynski⁵ and Boswarva, Howard, and Lidiard.⁷ Macfarlane, McLean, Quarrington, and Roberts¹⁰ have measured the detailed shape of the absorption edge in germanium in zero magnetic field and find that it is modified by exciton effects in the manner predicted by Elliott.⁹ At 249°K, where $kT \gg \hbar\omega_{ex}$, their data show a well-developed exciton line merging into the continuum absorption which is also modified by Coulomb binding effects in the immediate vicinity of the energy gap E_g . At 291°K the discrete line has merged with the background absorption; however, the absorption in the edge region still clearly differs from that expected for direct allowed interband transitions neglecting the coulomb interaction of electron and holes.

The modification of the transitions at the band edge by Coulomb effects in zero magnetic field is expected to produce a corresponding modification in the Faraday rotation in the immediate vicinity of the band edge. On the other hand, since the Coulomb effects are not apparent in the absorption well above the band edge, the Faraday rotation well below the band edge is not expected to exhibit such effects.

We utilize these considerations concerning the transitions at the band edge to tentatively explain the detailed structure of the Faraday rotation presented in

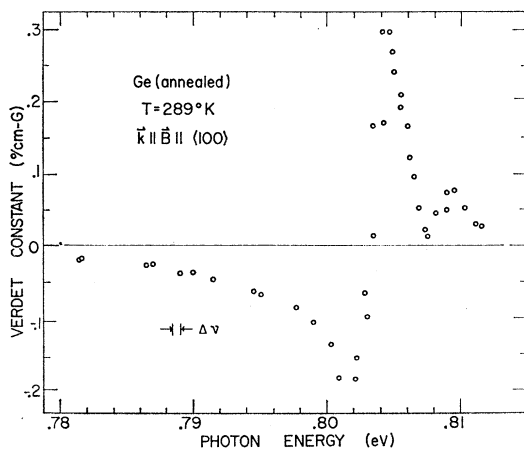


FIG. 3. Verdet constant of germanium measured in the vicinity of the zero-field band edge.

Fig. 3. The rotation, measured in this region, exhibits a central spike superposed on a dispersion curve. We associate the central spike with the splitting of the main discrete exciton line in the magnetic field, and the dispersion curve we associate with the splitting of the continuum absorption edge. The centers of these superposed curves lie at (0.8045 ± 0.001) eV and (0.8055 ± 0.001) eV which are approximately 1 meV below the values obtained by Macfarlane, McLean, Quarrington, and Roberts¹⁰ for the exciton transition energy and continuum edge, respectively.

V. STRONG MAGNETIC FIELDS

A. Exciton Transitions

Treatments of the interband Faraday rotation in terms of transitions between Landau levels are not expected to be correct in all details for the case of large magnetic fields. Elliott and Loudon¹¹ have studied the transitions between bound exciton states in the approximation that the cyclotron energy is large compared to the binding energy of the exciton. They find that these transitions become increasingly important with increasing field and become dominant for moderate values of magnetic field for materials with small effective masses. In germanium their approximation becomes valid at fields above 5–10 kG.

These conclusions are borne out by measurements of the ellipticity produced by large magnetic fields. A recorder trace of the ellipticity measured at 86 kG is shown in Fig. 4. The scale has been adjusted to read amplitude ellipticity which may be related to the differential absorption ($\alpha_+ - \alpha_-$) by Eq. (3.2).

Similar results are obtained by combining independent measurements of the absorption for (lcp) and (rcp) radiation obtained from the ordinary interband magneto-optical absorption measurements. This may be observed by taking the difference between the absorption curves for (lcp) and (rcp) radiation given by Burstein, Picus, Wallis, and Blatt.¹⁶ From these curves it may be observed that the line at lowest energy is stronger for (lcp) than for (rcp) radiation and that the two are separated by less than the relaxation broadening. Combining the two leads to a line such as the measured line labeled (1') which indicates the dominance of the (1cp) absorption. Similarly, the higher IMO absorption terms may be combined to give the ellipticity curve presented here.

The shapes of these absorption terms are characteristic of discrete transitions and do not show the tails to higher frequency expected for Landau transitions. In particular, we have calculated the line shape expected for the line labeled (1') on the basis of Landau transitions. We have used the valence band parameters given by Wallis and Bowlden¹⁷ and the calculated intensities

¹⁶ E. Burstein, G. S. Picus, R. F. Wallis, and F. Blatt, Phys. Rev. **113**, 15 (1959).

¹⁷ R. F. Wallis and H. J. Bowlden, Phys. Rev. **118**, 456 (1960).

given by Burstein, Picus, Wallis, and Blatt.¹⁶ The lowest line (1') is composed of transitions from each of the four valence bands. The resulting line is dominated by transitions from the ϵ_2^+ level and has an asymmetric shape which is not consistent with the experimental curve. A similar calculation utilizing the exciton line shape given by Elliott and Loudon¹¹ does reproduce the essential features of the experimental curve.

B. Application of Dispersion Relations

The dispersion relationship between the Faraday rotation and ellipticity may be observed in the recorder traces presented in Fig. 4. Each major absorption term is reflected in the rotation curve as a dispersion curve centered at the same frequency as the absorption line. The minor features are also fairly well reproduced, e.g.,

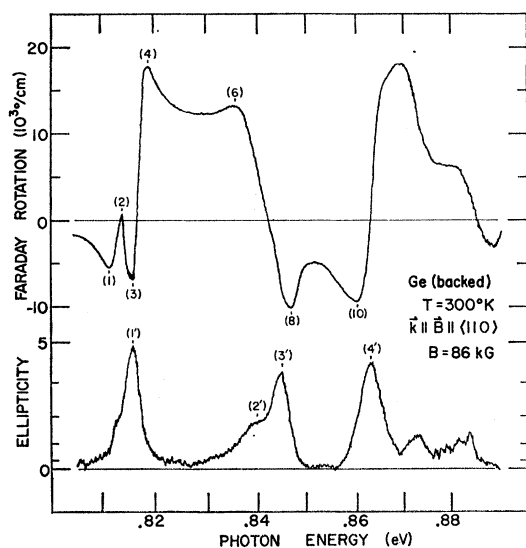
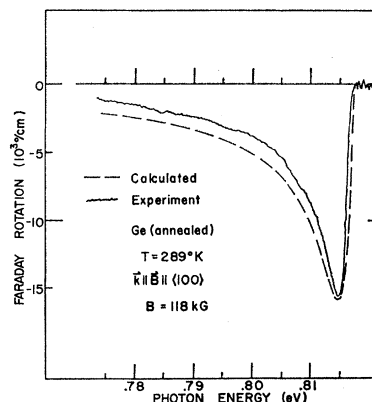


FIG. 4. Recorder traces for the Faraday rotation and ellipticity measured with the same sample of germanium. The sample thickness was 5.72μ . The extrema are labeled with numbers for purposes of identification.

the shoulder on the lowest ellipticity line is reflected in the rotation as the minor structure observed at lowest frequency. Since we measure only the absolute magnitude of ellipticity, its sign must be determined by the sense of the rotation.

The magnitudes of the measured rotation and ellipticity curves may also be compared by the dispersion relation Eq. (3.3). For an approximate calculation we assume a Lorentzian line shape for the line labeled (1') in Fig. 4. Taking values for the peak value and half-width from the ellipticity curve we calculate a value for the peak-to-peak rotation associated with this line. The calculated value is 10% greater than the corresponding measured value. The line labeled (4') also gives agreement to within 10%. Numerically integrating the entire curve should improve the agreement.

FIG. 5. Recorder trace of the Faraday rotation for photon energies below the high-field band edge. The dashed line represents the frequency dependence calculated for a discrete exciton transition.



C. Experimental Results

1. Frequency Dependence

A recorder trace of the rotation measured in an annealed and freely mounted sample is shown in Fig. 5. The annealed sample showed no evidence of the minor structure observed in mounted samples as in Fig. 4. The curve in Fig. 5 should represent the frequency dependence of the rotation arising from only the transitions at lowest frequency (1' of Fig. 4) since at these large magnetic fields (118 kG) the higher transitions have been shifted to much higher energy and the dispersion tails arising from these transitions will be small. The major contribution to this lowest set of transitions arises from the ϵ_2^+ transition.

Although the lowest set of transitions is dominated by the strong ϵ_2^+ transition, the presence of the weaker transitions should slightly increase the frequency dependence of the observed rotation. It may be observed that the measured rotation does have a slightly stronger frequency dependence than is given by the rotation arising from a single discrete term.

2. Field Dependence of Amplitude

The field dependence of the peak value of the ellipticity for the line at lowest frequency is shown in Fig. 6.

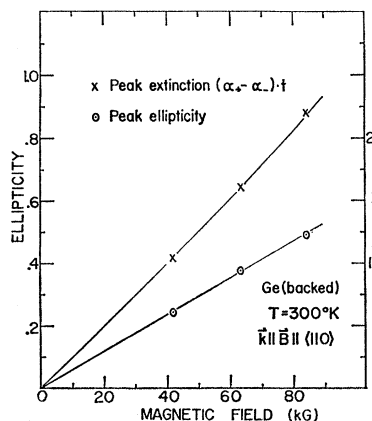


FIG. 6. Peak amplitude of the ellipticity and differential absorption factor $(\alpha_+ - \alpha_-)t$ plotted as a function of the magnetic field. The peak corresponds to that labeled (1') in Fig. 4.

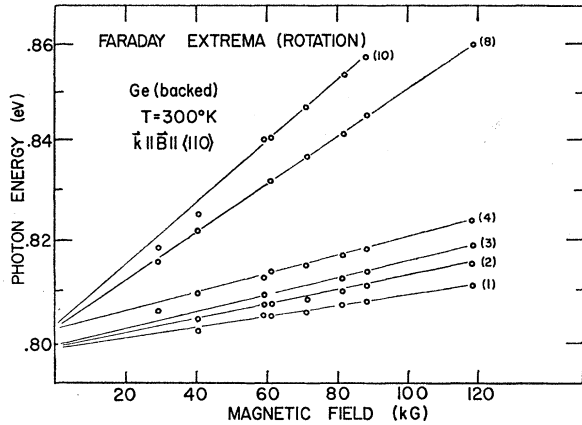


FIG. 7. Position in energy of the Faraday rotation peaks plotted as a function of the magnetic field. The numbered curves are identified in Fig. 4.

Also shown is the field dependency of the $(\alpha_+ - \alpha_-)$ term calculated from the ellipticity using Eq. (3.2). According to Elliott and Loudon,¹¹ the strength of the lowest exciton transition should increase with magnetic field as some power slightly greater than unity. The observed departure from linearity in Fig. 6 is in the proper direction.

3. Field Dependence of Position

The position in energy of the peaks observed in rotation are presented in Fig. 7 as a function of the applied field. The ellipticity extrema are plotted in Fig. 8. A linear shift with field for strong fields is observed in each case. Extrapolating the positions of the extrema to zero field, we obtain a value of (0.803 ± 0.001) eV for the upper sets of transitions and (0.800 ± 0.001) eV for the lowest set of transitions. Note that these values are obtained with a sample with backing and may not be characteristic of strain-free material. Also the significance of the difference in these extrapolated values is not completely obvious. A contributing factor is the variation of the exciton binding energy with increasing Landau quantum number.

D. Strong-Field Saturation

Figure 9 presents recorder traces of the Faraday rotation for several fixed photon energies in the vicinity of

$$\theta_n(\omega_g) = -\frac{2\pi e^2 l}{n_0 c m} \left[\frac{A_n^+}{(\beta_n + \gamma_n)[2\omega_g + (\beta_n + \gamma_n)H]} - \frac{A_n^-}{(\beta_n - \gamma_n)[2\omega_g + (\beta_n - \gamma_n)H]} \right]. \quad (5.2)$$

Each term is essentially independent of magnetic field over a range of n and H such that $\omega_{ex} \ll (\beta_n \pm \gamma_n)H \ll 2\omega_g$. At large n the quantities A_n^\pm may be assumed to a good approximation to be independent of both n and H . An upper bound on the contribution to the rotation from transitions with large n may then be obtained by re-

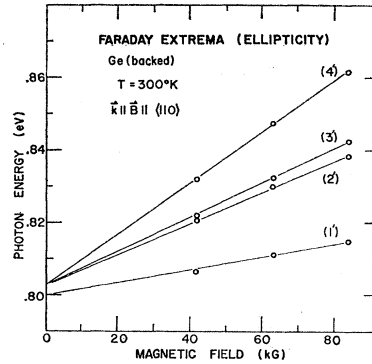


FIG. 8. Position in energy of the Faraday ellipticity peaks plotted as a function of the magnetic field. The numbered curves are identified in Fig. 4.

the zero-field energy gap. The curves all tend to saturate at large magnetic fields. The central trace (b) is essentially constant for magnetic fields larger than 20 kG while the other curves (a) and (c) tend to approach the central curve at large fields.

This behavior is consistent with a simplified model based on the exciton theory of Elliott and Loudon.¹¹ At large magnetic fields ($\omega_{ex} \ll \omega_c$) they find that the transition to the lowest bound exciton state, associated with a given Landau level, is dominant while the transitions to excited states of the exciton and to the continuum are negligible. They also find that the f values for the transitions have a magnetic-field dependence that is approximately linear and of the form $f_n = A_n H^x / \omega_n$, where $x \approx 1$. The factor A_n represents a combination of constants and ω_n the frequency for the transition.

With this form for the f values and with $\omega = \omega_g$, Eq. (3.10) of Boswarva, Howard, and Lidiard⁷ may be written

$$\theta(\omega_g) = -\frac{2\pi e^2 l H}{n_0 c m} \sum_n \left[\frac{A_n^+}{(\omega_n^+)^2 - \omega_g^2} - \frac{A_n^-}{(\omega_n^-)^2 - \omega_g^2} \right], \quad (5.1)$$

where $\omega_n^\pm = \omega_g + (\beta_n \pm \gamma_n)H$. The factors β_n and γ_n represent the cyclotron and gyromagnetic factors for the transition. The exciton binding frequency has been neglected in the expression for ω_n^\pm since it is small compared to $(\beta_n \pm \gamma_n)H$ at the large fields being considered.

At low n , where quantum effects are expected, the terms may be treated individually. Expanding the denominator in Eq. (5.1), the contribution to the rotation for a given n may be written

placing the sum over n by a suitable integral. One finds that this contribution does indeed saturate under conditions appropriate to germanium in magnetic fields around 100 kG. Combining the contributions from small and large n leads to a rotation which saturates in agreement with the experimental data.

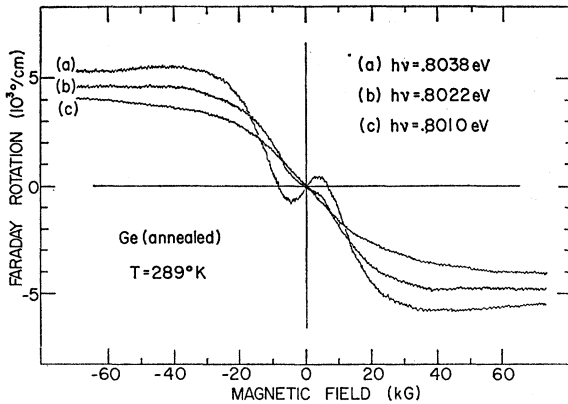


FIG. 9. Recorder traces of the Faraday rotation in germanium as a function of the magnetic field. The fixed photon energies lie in the vicinity of the zero-field band edge.

E. Effects in Crystal Strain

The Faraday rotation for a thin section of germanium mounted on a glass backing is shown in Fig. 10. The second trace was obtained with the sample rotated by 180° so that the orientation of the glass backing relative to the germanium was interchanged. The altered structure observed is not possible for a crystal with a center of symmetry. The presence of these effects is direct evidence of the removal of the center of symmetry in the germanium due to the presence of crystal strain. Corresponding differences were observed in the measured ellipticity by reversal of the sample.

The presence of strain in thin crystals mounted on a backing is not unexpected. In fact, we observed such effects in all crystals measured which were mounted on a backing. Less expected was the presence of strain effects in a $\langle 110 \rangle$ oriented crystal which was annealed for 1 h at 600°C and freely mounted. It is possible that the residual strain in this crystal is due to screw dislocations introduced during the growth of the crystal. One crystal with its normal oriented along the $\langle 100 \rangle$ crystal axis showed no evidence of crystal strain. The data obtained with this sample are labeled Ge (annealed).

VI. CONCLUSIONS

Effects which appear to arise from the Coulomb interaction of holes and electrons are observed in the interband Faraday rotation in germanium for both weak and strong magnetic fields. In weak magnetic fields ($\omega_c\tau \ll 1$ and $\omega_c \ll \omega_{ex}$) the rotation at photon energies near the band edge ($\hbar\omega < \hbar\omega_g$) shows a departure from the behavior expected neglecting the Coulomb interaction of the holes and electrons.

The Faraday rotation in strong magnetic fields

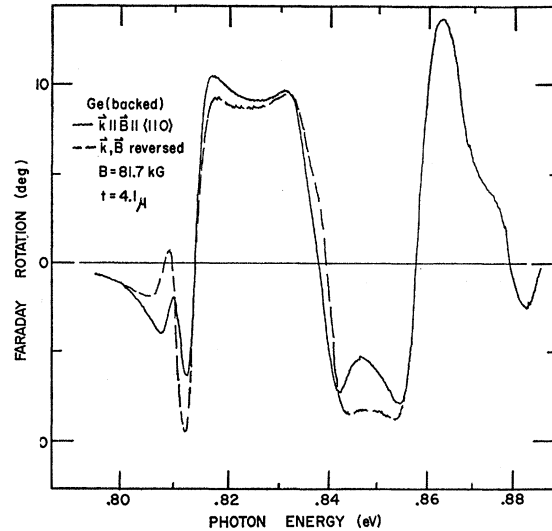


FIG. 10. Faraday rotation for a germanium section mounted on a glass backing. The second trace was produced with a sample rotated 180° about an axis perpendicular to the magnetic field.

($\omega_c\tau > 1$ and $\omega_c > \omega_{ex}$) exhibits structure at photon energies above the band edge ($\hbar\omega > \hbar\omega_g$). A corresponding structure is also observed in the ellipticity measured in strong magnetic fields. The detailed field and energy dependences of the observed structure are in accord with a model based on transitions between discrete exciton levels. This model also predicts a saturation of the Faraday rotation when measured at a photon energy equal to the zero-field band-gap energy ($\hbar\omega = \hbar\omega_g$). This saturation is observed experimentally.

The sensitivity of these measurements to crystal strain are an indication of the extreme caution that must be taken in the preparation of samples for measurement. Thin crystal sections mounted on a backing are suspect even at room temperature. Annealed and freely mounted crystals may also not be free from strain. Conversely, the sensitivity of these measurements to crystal strain make this a useful tool for the study of strain effects in solids.

ACKNOWLEDGMENTS

Much of the optical instrumentation for these measurements was developed by E. D. Palik who also assisted in many of the experiments.

Our appreciation is also extended to W. C. Sadler for performing the x-ray orientation studies and to A. Mister, R. Anonsen, W. Cline, and J. Donnelly for providing the large fields essential to these measurements. One of the authors (D. L. M.) wishes to acknowledge fruitful conversations with R. E. Howard and E. A. Stern and correspondence with A. B. Lidiard.